

A point mutation in the Ncr1 signal peptide impairs the development of innate lymphoid cell subsets.

Francisca F. Almeida, Sara Tognarelli, Antoine Marcais, Andrew J. Kueh, Miriam E. Friede, Yang Liao, Simon N. Willis, Kylie Luong, Fabrice Faure, Francois E. Mercier, et al.

▶ **To cite this version:**

Francisca F. Almeida, Sara Tognarelli, Antoine Marcais, Andrew J. Kueh, Miriam E. Friede, et al.. A point mutation in the Ncr1 signal peptide impairs the development of innate lymphoid cell subsets.. OncoImmunology, 2018, 7 (10), pp.e1475875. 10.1080/2162402X.2018.1475875 . hal-02086847

HAL Id: hal-02086847
https://amu.hal.science/hal-02086847

Submitted on 1 Apr 2019

HAL is a multi-disciplinary open access archive for the deposit and dissemination of scientific research documents, whether they are published or not. The documents may come from teaching and research institutions in France or abroad, or from public or private research centers.

L'archive ouverte pluridisciplinaire **HAL**, est destinée au dépôt et à la diffusion de documents scientifiques de niveau recherche, publiés ou non, émanant des établissements d'enseignement et de recherche français ou étrangers, des laboratoires publics ou privés.



Distributed under a Creative Commons Attribution - NonCommercial - NoDerivatives 4.0 International License



OncoImmunology

ISSN: (Print) 2162-402X (Online) Journal homepage: https://www.tandfonline.com/loi/koni20

A point mutation in the *Ncr1* signal peptide impairs the development of innate lymphoid cell subsets

Francisca F. Almeida, Sara Tognarelli, Antoine Marçais, Andrew J. Kueh, Miriam E. Friede, Yang Liao, Simon N. Willis, Kylie Luong, Fabrice Faure, Francois E. Mercier, Justine Galluso, Matthew Firth, Emilie Narni-Mancinelli, Bushra Rais, David T. Scadden, Francesco Spallotta, Sandra Weil, Ariane Giannattasio, Franziska Kalensee, Tobias Zöller, Nicholas D. Huntington, Ulrike Schleicher, Andreas G. Chiocchetti, Sophie Ugolini, Marco J. Herold, Wei Shi, Joachim Koch, Alexander Steinle, Eric Vivier, Thierry Walzer, Gabrielle T. Belz & Evelyn Ullrich

To cite this article: Francisca F. Almeida, Sara Tognarelli, Antoine Marçais, Andrew J. Kueh, Miriam E. Friede, Yang Liao, Simon N. Willis, Kylie Luong, Fabrice Faure, Francois E. Mercier, Justine Galluso, Matthew Firth, Emilie Narni-Mancinelli, Bushra Rais, David T. Scadden, Francesco Spallotta, Sandra Weil, Ariane Giannattasio, Franziska Kalensee, Tobias Zöller, Nicholas D. Huntington, Ulrike Schleicher, Andreas G. Chiocchetti, Sophie Ugolini, Marco J. Herold, Wei Shi, Joachim Koch, Alexander Steinle, Eric Vivier, Thierry Walzer, Gabrielle T. Belz & Evelyn Ullrich (2018) A point mutation in the *Ncr1* signal peptide impairs the development of innate lymphoid cell subsets, OncoImmunology, 7:10, e1475875, DOI: 10.1080/2162402X.2018.1475875

To link to this article: https://doi.org/10.1080/2162402X.2018.1475875

© 2018 The Author(s). Published by Taylor & Francis.

View supplementary material

Published online: 15 Aug 2018.

Submit your article to this journal

Article views: 620

View Crossmark data

Citing articles: 1 View citing articles

Full Terms & Conditions of access and use can be found at
https://www.tandfonline.com/action/journalInformation?journalCode=koni20

ONCOIMMUNOLOGY
2018, VOL. 7, NO. 10, e1475875 (15 pages)
https://doi.org/10.1080/2162402X.2018.1475875

Taylor & Francis
Taylor & Francis Group

ORIGINAL RESEARCH

Check for updates

A point mutation in the *Ncr1* signal peptide impairs the development of innate lymphoid cell subsets

Francisca F. Almeida [a,b], Sara Tognarelli[c,d], Antoine Marçais[e], Andrew J. Kueh[a,b], Miriam E. Friede[f], Yang Liao[a,b], Simon N. Willis[a,b], Kylie Luong[a,b], Fabrice Faure[e], Francois E. Mercier[g], Justine Galluso[h], Matthew Firth[a,b], Emilie Narni-Mancinelli[h], Bushra Rais[c,d], David T. Scadden[i], Francesco Spallotta[j], Sandra Weil[k,l], Ariane Giannattasio[k,l], Franziska Kalensee[c,d], Tobias Zöller[f], Nicholas D. Huntington[a,b], Ulrike Schleicher[m], Andreas G. Chiocchetti[n], Sophie Ugolini [h], Marco J. Herold[a,b], Wei Shi[a,o], Joachim Koch[k,l], Alexander Steinle [f], Eric Vivier [h,p,q], Thierry Walzer[e], Gabrielle T. Belz [a,b], and Evelyn Ullrich [d,c]

[a]Division of Molecular Immunology, Walter and Eliza Hall Institute of Medical Research, Melbourne, Victoria, Australia; [b]Department of Medical Biology, University of Melbourne, Melbourne, Victoria, Australia; [c]Division of Stem Cell Transplantation and Immunology, Department for Children and Adolescents Medicine, Johann Wolfgang Goethe University Hospital, Frankfurt am Main, Germany; [d]LOEWE Center for Cell and Gene Therapy, Johann Wolfgang Goethe University, Frankfurt am Main, Germany; [e]CIRI, Centre International de Recherche en Infectiologie - International Center for Infectiology Research, Inserm, U1111, CNRS, UMR5308, Ecole Normale Supérieure de Lyon, Université Lyon 1, Lyon, France; [f]Institute for Molecular Medicine, Johann Wolfgang Goethe University, Frankfurt am Main, Germany; [g]Department of Medicine, McGill University, Montreal, Quebec, Canada; [h]CNRS, INSERM, CIML, Centre d'Immunologie de Marseille-Luminy, Aix Marseille University, Marseille, France; [i]Harvard Stem Cell Institute, Cambridge, MA, USA; [j]Division of Cardiovascular Epigenetics, Department of Cardiology, Johann Wolfgang Goethe University, Frankfurt am Main, Germany; [k]Georg Speyer Haus, Institute for Tumor Biology and Experimental Therapy, Frankfurt am Main, Germany; [l]Institute of Medical Microbiology and Hygiene, University of Mainz Medical Center, Mainz, Germany; [m]Mikrobiologisches Institut-Klinische Mikrobiologie, Immunologie und Hygiene, Friedrich-Alexander-Universität Erlangen-Nürnberg und Universitätsklinikum Erlangen, Erlangen, Germany; [n]Molecular Genetics Laboratory, Department for Child and Adolescent Psychiatry, Psychosomatics and Psychotherapy, Johann Wolfgang Goethe University, Frankfurt am Main, Germany; [o]Department of Computing and Information Systems, University of Melbourne, Melbourne, Victoria, Australia; [p]Innate Pharma, Marseille, France; [q]Service d'Immunologie, Hôpital de la Timone, Marseille Immunopole, Assistance Publique - Hôpitaux de Marseille, Marseille, France

ABSTRACT

NKp46 (CD335) is a surface receptor shared by both human and mouse natural killer (NK) cells and innate lymphoid cells (ILCs) that transduces activating signals necessary to eliminate virus-infected cells and tumors. Here, we describe a spontaneous point mutation of cysteine to arginine (C14R) in the signal peptide of the NKp46 protein in congenic Ly5.1 mice and the newly generated NCR^{B6C14R} strain. Ly5.1^{C14R} NK cells expressed similar levels of *Ncr1* mRNA as C57BL/6, but showed impaired surface NKp46 and reduced ability to control melanoma tumors *in vivo*. Expression of the mutant NKp46^{C14R} in 293T cells showed that NKp46 protein trafficking to the cell surface was compromised. Although Ly5.1^{C14R} mice had normal number of NK cells, they showed an increased number of early maturation stage NK cells. CD49a^{+}ILC1s were also increased but these cells lacked the expression of TRAIL. ILC3s that expressed NKp46 were not detectable and were not apparent when examined by T-bet expression. Thus, the C14R mutation reveals that NKp46 is important for NK cell and ILC differentiation, maturation and function.

Significance

Innate lymphoid cells (ILCs) play important roles in immune protection. Various subsets of ILCs express the activating receptor NKp46 which is capable of recognizing pathogen derived and tumor ligands and is necessary for immune protection. Here, we describe a spontaneous point mutation in the signal peptide of the NKp46 protein in congenic Ly5.1 mice which are widely used for tracking cells *in vivo*. This *Ncr1* C14R mutation impairs NKp46 surface expression resulting in destabilization of *Ncr1* and accumulation of NKp46 in the endoplasmic reticulum. Loss of stable NKp46 expression impaired the maturation of NKp46^{+} ILCs and altered the expression of TRAIL and T-bet in ILC1 and ILC3, respectively.

ARTICLE HISTORY
Received 7 May 2018
Accepted 7 May 2018

KEYWORDS
innate lymphoid cells; activation receptors; intracellular trafficking; congenic mice

Introduction

Natural killer (NK) cells are cytolytic and cytokine-producing cells that contribute to eradicate pathogen-infected cells and cancers thereby mediating frontline defense and immunosurveillance.[1,2] The capacity to mediate these functions depends on the balance between inhibitory and activating signals. Activating receptors include the family of natural

CONTACT Gabrielle T. Belz belz@wehi.edu.au; Evelyn Ullrich Evelyn.Ullrich@kgu.de Walter and Eliza Hall Institute of Medical Research, Melbourne, Victoria, 3052, Australia; Division of Stem Cell Transplantation and Immunology, Department for Children and Adolescents Medicine, Johann Wolfgang Goethe University Hospital, Frankfurt am Main, Germany

F.F.A and S.T. contributed equally and G.T.B. and E.U. contributed equally.
Color versions of one or more of the figures in the article can be found online at www.tandfonline.com/koni.
Supplemental data for this article can be accessed here.

© 2018 Taylor & Francis Group, LLC

cytotoxicity receptors (NCRs) NKp46, NKp30 and NKp44.[3,4] NKp46 is expressed by NK cells and group 1 and 3 innate lymphoid cells (ILCs).[5-7] NKp46 is encoded by *Ncr1* and associates with the ITAM-containing CD3ζ or FcRγ polypeptides. Several endogenous ligands of NKp46 have been described including the complement factor P,[8] the intracellular filamentous cytoskeletal protein vimentin expressed on the surface of *Mycobacterium tuberculosis*–infected monocytes,[9] and several viral proteins such as hemagglutinin and hemagglutinin neuraminidases of the influenza,[10,11] Sendai,[12] Newcastle disease,[13] ectromelia and vaccinia viruses.[14] NKp46 was also shown to recognize PfEMP1 of *Plasmodium falciparum*,[14] an unknown ligand from *Fusobacterium nucleatum*,[15] adhesins from *Candida glabrata*.[16] This wide expression supports that the triggering of NKp46 is essential for effective immune responses.

Previous studies have shown that mutations of the *Ncr1* gene can cause a reduction in the cell surface expression of the NKp46 protein. Various strains of mice have been generated that either lack *Ncr1* or exhibit mutations that have been chemically induced.[12,17,18] These lines ($Ncr^{gfp/gfp}$, $Ncr1^{Noe/Noe}$ and $Ncr1^{iCre/iCre}$) exhibit different phenotypes, possibly as a consequence of their difference in NKp46 protein expression. For example, $Ncr1^{Noe/Noe}$ and $Ncr1^{iCre/iCre}$ strains harbor modest gene changes but preserve the protein while $Ncr1^{gfp/gfp}$ mice,[17] and $Ncr1^{gfp/gfp}Klrk1^{-/-}$ double knockout mice which have defects in both NKp46 and NKG2D expression,[19] lack exons 5–7 resulting in a complete disruption of the protein.

Narni-Mancinelli et al.[18] first described the effect of the point mutation W32R in a colony of C57BL/6J mice carrying N-ethyl-N-nitrosourea (ENU)–induced mutations (called *Noé* mice). These mice had normal numbers of NK cells but showed an impaired expression of NKp46 on the cell surface. Moreover, *Noé* mice displayed an increased expression of the zinc-finger protein *Helios* which is involved in the regulation of lymphocyte development. *Noé* NK cells were hyper responsive to various stimuli *in vitro* and *Noé* mice were more resistant to infection with mouse cytomegalovirus.[18] Glasner *et al.*[20] further characterized the effect of the *Noé* mutation clarifying that the $NKp46^{W32R}$ protein could reach the surface of NK cells, but in a slow and unstable manner. This resulted in an accumulation of NKp46 in the endoplasmic reticulum (ER) and limited transport to the cell surface.[20] Recently, studies of human NK cells carrying the same mutation $NKp46^{W32R}$ led to similar conclusions.[21]

Here we describe the analysis of two independent colonies of congenic $CD45.1^+$ (Ly5.1) mice that exhibited a spontaneous single point mutation (C14R, designated $Ly5.1^{C14R}$ mice) in the signal sequence of the *Ncr1* gene. This mutation impaired NKp46 surface expression in ILC subsets. The C14R mutation did not alter the overall expression of *Ncr1* mRNA in mutant NK cells but impaired the surface expression of NKp46 in ILCs and was associated with alteration in ILC maturation. These results were also confirmed by a newly generated NCR^{B6C14R} strain.

Results

Ly5.1 congenic mouse strains exhibit a reduced surface expression of NKp46

Ly5.1 (*B6.SJL-Ptprca Pepcb/BoyJ*) congenic mice expressing CD45.1 on the surface of all lymphocytes are classically used in combination with CD45.2-expressing C57BL/6 mice to establish experimental systems in which donor and host immune cells can be faithfully tracked both at steady-state and during an immune challenge. However, during analyses of these types of systems, it was noticed that $Ly5.1^+$ mice consistently exhibited very poor expression of the receptor NKp46, a key phenotypic marker of NK cells[22] and some subsets of ILCs, in multiple tissues including peripheral blood (Figure 1A), bone marrow, peripheral lymph nodes and spleen (Figure 1B). This observation was made in two mouse colonies completely independent of each other but which were originally derived from the Jackson Laboratory (Jax) imported in 2008 (University Hospital Erlangen) and 2010 (Walter and Eliza Hall Institute, WEHI) and maintained as closed colonies. This was distinct from newly imported mice (2012, University Hospital Erlangen; 2016, WEHI), also from Jax, which exhibited NKp46 expression equivalent to the C57BL/6 lines and F1 mice derived from the originally imported Ly5.1 line (C57BL/6 × Ly5.1WEHI) (SI Appendix, Figure S1A). These findings suggested that this alteration was a recessive trait limited to specific colonies that may have carried the mutation. While this mutation was tightly linked to the *Ptprca* locus on chromosome 1, *Ncr1* is found on chromosome 7 indicating that the alteration was not within *Ptprca* itself.

A single amino acid change in the Ncr1 gene abrogates stable NKp46 surface expression

To understand the basis of this alteration, we used whole exome sequencing to examine C57BL/6 Ly5.1 (WEHI) and Ly5.1 (WEHI) from the mouse colonies in Melbourne, Australia. Assuming a recessive pattern of inheritance, 1042 SNPs were identified that were homozygous in the affected mice and heterozygous in the parental strain (SI Appendix, Dataset S1). Of these, 670 SNPs were classified as low impact mutations based on variant effector predictor analysis and as such were excluded from further analysis. Based on the observed phenotype, we initially concentrated on the candidate gene *Ncr1*. NKp46 is a 46 kDa type 1 transmembrane glycoprotein characterized by a short intracellular tail, a single transmembrane domain, and two extracellular Ig-like domains. Sequence analysis identified a single homozygous missense point mutation (T to C) in the signal peptide of *Ncr1* in both strains of mice that exhibited low NKp46 protein expression. We confirmed by Sanger sequencing that the mutation was present in Ly5.1 WEHI (hereinafter referred to as $Ly5.1^{C14R}$) mice and C57BL/6 × $Ly5.1^{C14R}$ but not C57BL/6 mice and resulted in a single amino acid substitution of cysteine to arginine (C14R; Figure 1C). In contrast, the RNA level of *Ncr1* did not significantly differ in NK cells from C57BL/6, $Ly5.1^{C14R}$, WT Ly5.1 and C57BL/6 × $Ly5.1^{C14R}$ mice (Figure 1D). It should be noted that subsequent to identification of this mutation in the established lines at each institution, new founders were imported to the WEHI (2016) to establish a new 'unmutated' colony. Breedings were kept entirely separate from the original colonies and progeny from the new breedings were analysed. Of these, 39 of 88 mice tested exhibited a reduction in NKp46 expression by

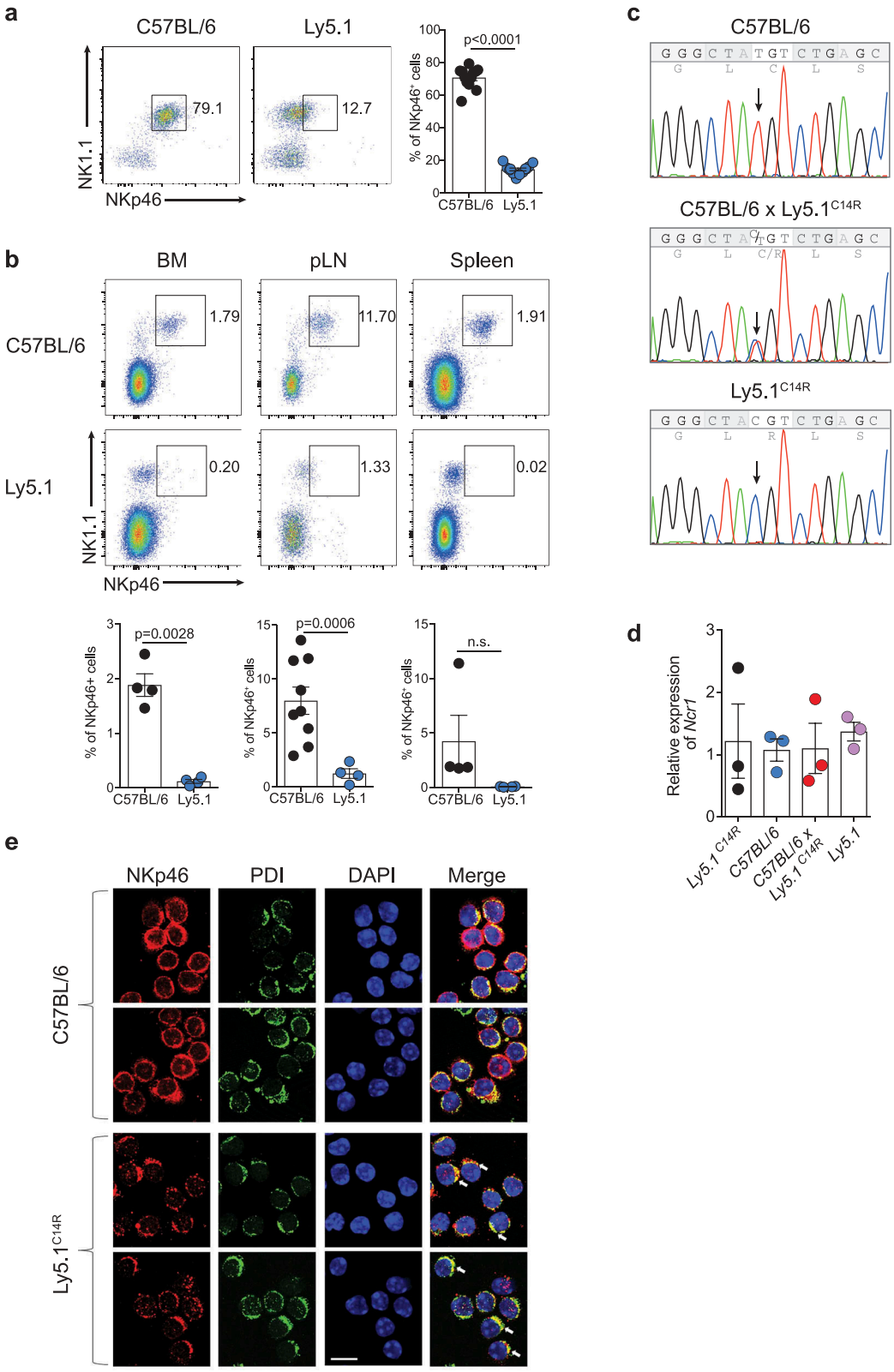


Figure 1. Ly5.1 congenic mouse strain exhibits reduced surface expression of NKp46 that alters the localization of the NKp46 protein. (A) Dot plot showing the staining and frequency of NK1.1^{+}NKp46^{+} cells in the peripheral blood lymphocytes of C57BL/6 and Ly5.1 mice. Data show representative plots gated on live lymphocytes CD3^{-} CD19^{-} (n = 12 mice/genotype). (B) Dot plots showing the expression and frequency quantification of NK1.1^{+}NKp46^{+} cells in the bone marrow (BM), peripheral lymph node (pLN) and spleen of C57BL/6 and Ly5.1 mice. (A, B) Data show representative plots gated on live lymphocytes CD3^{-}CD19^{-} pooled from two to five independent experiments (n = 4–12 mice/genotype/tissue). (C) Sanger sequencing analysis of the *Ncr1* gene in C57BL/6, C57BL/6 × Ly5.1^{C14R} and Ly5.1^{C14R} mice showing the position of the point mutation. (D) Relative levels of NKp46 transcripts in splenic NK cells of C57BL/6, Ly5.1^{C14R}, WT Ly5.1 and C57BL/6 × Ly5.1^{C14R} mice. Data show the mean ± SEM of 3–4 mice/genotype for one of three similar experiments. P values were calculated using an unpaired two-tailed Student's t test. (E) NKp46 localization in primary NK cells. Representative images of NK cells isolated from C57BL/6 and mutant Ly5.1^{C14R} mice stained with anti-NKp46 and anti-PDI primary antibodies, and AlexaFluor488-conjugated anti-goat and AlexaFluor546-conjugated anti-rabbit secondary antibodies (DAPI nuclear stain, blue; anti-NKp46, red; PDI, green). Images were obtained using confocal scanning microscopy. Arrows indicate ER localization. Scale bar, 10 µm.

flow cytometry.We further sequenced 29 mice from the new colony; 9 were homozygous wild-type for the *Ncr1* gene and were used to reestablish the colony while the remainder were heterozygous. Thus, it appears that the mutation has inadvertently been retained undetected long term in parent colonies.

The C14R Ncr1 mutation significantly impairs surface NKp46 expression in 293T cells

As the discovery that a mutation in the leader sequence might affect NKp46 cell surface expression or trafficking was unexpected, we sought to demonstrate that ectopic expression of the NKp46^{C14R} mutation itself was responsible for the alterations we observed in the mutated Ly5.1 mice. To this end, 293T cells were transfected with wild-type NKp46 or NKp46^{C14R} cDNA, respectively, and the expression of NKp46 was tracked by flow cytometry. The surface expression of the NKp46^{C14R} protein on 293T transfectants was significantly reduced compared with wild-type NKp46 while the total cellular NKp46 expression was at a comparable level (SI Appendix, Figure S1B and C), demonstrating that the impaired surface expression of NKp46 in Ly5.1 mice in fact is due to the C14R mutation in the NKp46 signal peptide. Analyses of freshly isolated naïve NK cells from wild-type or Ly5.1^{C14R} mice by confocal laser scanning microscopy not only confirmed the reduced NKp46^{C14R} surface localization, but also revealed a spotted intracellular distribution of the mutated NKp46^{C14R} protein. Furthermore, the colocalization of NKp46 with protein disulfide isomerase (PDI), an enzyme in the endoplasmic reticulum, indicated an accumulation of NKp46^{C14R} in that cell compartment (Figure 1E and SI Appendix, S1 *D*). Thus the C14R mutation in the signal peptide of NKp46^{C14R} resulted in disruption of NKp46 surface expression by failed trafficking within the cell.

Ly5.1^{C14R} mice have normal numbers of total NK cells but altered distribution of ILC subsets

We then interrogate if the C14R mutation might impact the subsets of cells that normally express NKp46, i.e. NK cells, ILC1 and NCR$^+$ ILC3s. Ly5.1^{C14R} mice exhibited normal numbers of NK1.1$^+$CD3$^-$ NK cells in the majority of the tissues but these numbers were significantly increased in the thymus compared with control mice (Figure 2A and B). We then examined the maturation status of NK cells by measuring the expression of KLRG1 and CD11b in C57BL/6 and Ly5.1^{C14R} NK cells (Figure 2C and D). This revealed an increase in the immature (Imm) NK cell subsets in the spleen but not in the liver of Ly5.1^{C14R} mice suggesting that steady-state signalling through NKp46 may act to modulate early NK cell maturation. Similar findings were observed when cells were analysed using CD27 and CD11b (SI Appendix, Figure S2A and B) and in Noé NK cells (SI Appendix, Figure S2C and D), a phenotype that was rescued by the expression of human NKp46.

ILC1 were identified through the expression of the CD49a integrin and of the absence of expression of the transcriptional regulator Eomesodermin (Eomes) which is required for the development of NK cells.[23] This showed that similar to NK cells, ILC1 were also enriched in the thymus (Figure 2E) although the level of expression of NKp46 in Ly5.1^{C14R} mice was reduced by ~3-fold for both populations across all tissues when compared to that found in C57BL/6 mice and ~1.5-fold for C57BL/6 × Ly5.1^{C14R} mice (Figure 2F). A similar reduction in the expression of NKp46 was seen in NK cells and ILC1s from tissues analysed in mixed bone marrow chimeras (SI Appendix, Figure S3). This effect was not seen in mice that carried only the six base pair mutation that encodes CD45.1 (CD45.1^{STEM}) (SI Appendix, Figure S4) demonstrating that the NKp46 expression defect in Ly5.1^{C14R} mice is intrinsic and not linked to Ly5.1 itself. In addition, hepatic ILC1 isolated from Ly5.1^{C14R} mice lacked expression of the TNF-related apoptosis-inducing ligand, TRAIL (encoded by *Tnfsf10*) normally characteristic of this population[24] (Figure 2G, *upper panels*). Such an effect was also seen in the *Ncr*$^{gfp/gfp}$ strain but not in Ly5.1^{STEM} mice (Figure 2G, *lower panels* and SI Appendix, S4 *B* and *C*).

To extend these analyses, we investigated how loss of NKp46 influenced NCR$^+$ and NCR$^-$ ILC3 subsets in the lamina propria (LP) and intraepithelial (IE) compartments of the small intestine (Figure 3). As expected, NCR$^+$ ILC3 were not detectable in the Ly5.1^{C14R} mice (Figure 3A and B) while ILC2 were present in normal numbers (data not shown). This was accompanied by an accumulation in both the frequency and number of NCR$^-$ ILC3. However, the overall number of Rorγt$^+$ ILC3 was similar suggesting that loss of NKp46 did not adversely affect the development of total ILC3 at steady-state. Nevertheless, analyses of T-bet expression revealed that it was upregulated within the NCR$^+$ subset in C57BL/6 mice as previously reported,[25,26] while NCR$^-$ ILC3 from Ly5.1^{C14R} mice did not show elevated levels of T-bet when compared with the NCR$^-$ population in C57BL/6 mice suggesting that NCR$^+$ cells fail to develop (Figure 3C).

Ly5.1^{C14R} mice have an altered sensitivity to stimuli in vitro and fail to control tumors in vivo

To gain insight on the functional relevance of the C14R point mutation, the degranulation capacity of total NK cells from C57BL/6 and Ly5.1^{C14R} mice was determined by staining for surface CD107a expression following exposure to various stimuli *in vitro*. As might be expected, NK cells from NKp46^{C14R} mice were significantly less responsive to NKp46 stimulation. When NK cells were cross-linked through NK1.1, they showed a trend towards increased degranulation which was not statistically significant on the whole NK cell population (Figure 4A), but was statistically significant when restricted to the immature NK cell subset (SI Appendix, Figure S5), consistent with previous findings on *Noé* mice.[18] Regardless of this point, however, the *in vitro* anti-tumor NK cell cytolytic capacity was intact in NK cells from Ly5.1^{C14R} mice (Figure 4B and SI Appendix, Figure S5). Combined, these data suggest that NKp46^{C14R} NK cells are functionally competent and can induce cell lysis through multiple pathways but exhibit defects *in vitro* when recognition requires engagement of NKp46.

These findings suggested that despite the alteration of NKp46 in Ly5.1^{C14R}, NK cells should be competent to protect against *in vivo* tumor challenge. To test this point, mice were inoculated with B16F10 melanoma cells which are known to be controlled by NK cells.[27,28] While C57BL/6, C57BL/6 × Ly5.1^{C14R} and Ly5.1 (Jax, 2017) mice were able to largely control tumor growth as measured by the number of primary lung tumors 14 days after tumor inoculation (Figure 4C and D), mice that expressed the

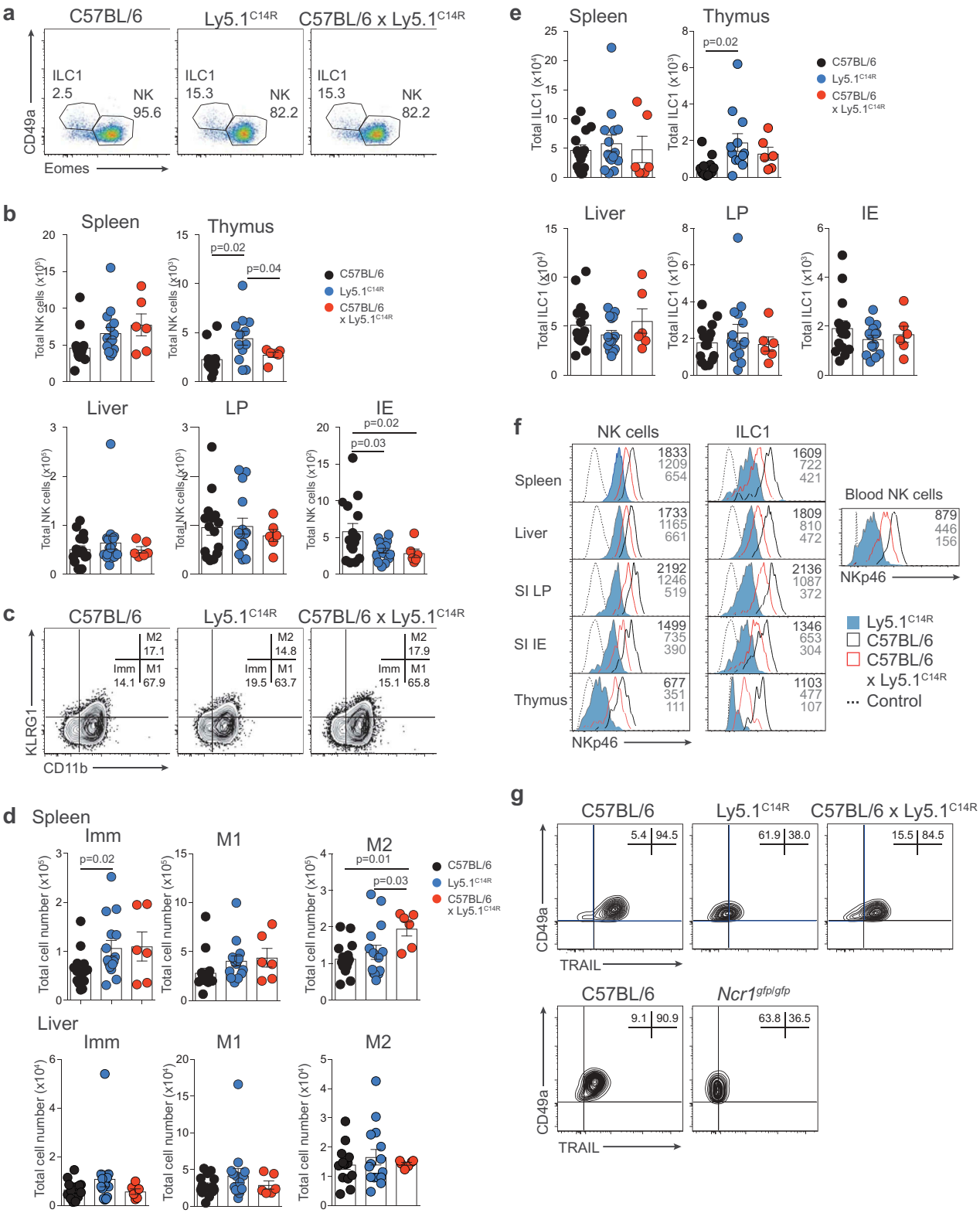


Figure 2. Disruption of NK cell homeostasis and maturation of ILC1 and NK cells in Ly5.1^{C14R} mice. (A) Dot plots showing the frequency of ILC1 and NK cells in the spleen. Data show representative plots gated on live NK1.1^{+} lymphocytes excluding T and B cells in C57BL/6, Ly5.1^{C14R} and C57BL/6 × Ly5.1^{C14R} mice. (B) Total number of NK cells in spleen, thymus, liver, small intestine lamina propria (LP) and within the intestinal intraepithelial compartment (IE). Data show the mean ± SEM pooled from three to six independent experiments (n = 6–15 mice/genotype); thymus are pooled from three to five independent experiments (n = 6–12 mice/genotype). P values were calculated using an unpaired two-tailed Student's t test. (C) FACS plots showing the frequency of immature (Imm, KLRG1^{-}CD11b^{-}), mature 1 (M1, KLRG1^{-}CD11b^{+}) and mature 2 (M2, KLRG1^{+}CD11b^{+}) NK cells in splenic NK1.1^{+}CD3^{-}CD19^{-} NK cells. (D) Total number of Imm, M1 and M2 NK cells in the spleen and liver of C57BL/6, Ly5.1^{C14R} and C57BL/6 × Ly5.1^{C14R} mice showing the mean ± SEM pooled from three to six independent experiments (n = 6–15 mice/genotype). P values were calculated using an unpaired two-tailed Student's t test. (E) Total number of ILC1s in spleen, thymus, liver, small intestine lamina propria (LP) and within the intestinal intraepithelial compartment (IE). Data show the mean ± SEM pooled from three to six independent experiments (n = 6–15 mice/genotype); thymus data are pooled from three to five independent experiments (n = 6–12 mice/genotype). P values were calculated using an unpaired two-tailed Student's t test. (F) Histograms showing the mean fluorescence intensity of NKp46 in various tissues for both NK cells and ILC1 for wild-type (black solid line), Ly5.1^{C14R} (solid blue) and C57BL/6 × Ly5.1^{C14R} (red solid line). CD3ε^{+} cells were used as a control for NKp46 expression (black dashed line). Data are representative of tissues analyzed in (A–E). (G) Expression of TRAIL on NK1.1^{+}CD49a^{+}CD3^{-}CD19^{-} hepatic ILC1 in C57BL/6, Ly5.1^{C14R} and C57BL/6 × Ly5.1^{C14R} (*results shown in the upper panels*) and in C57BL/6 controls compared to *Ncr1*$^{gfp/gfp}$ (*results from experiment shown in the lower panels*). Data show representative plots from three to five independent experiments and indicate the the frequency of expression (n = 6–12 mice/genotype).

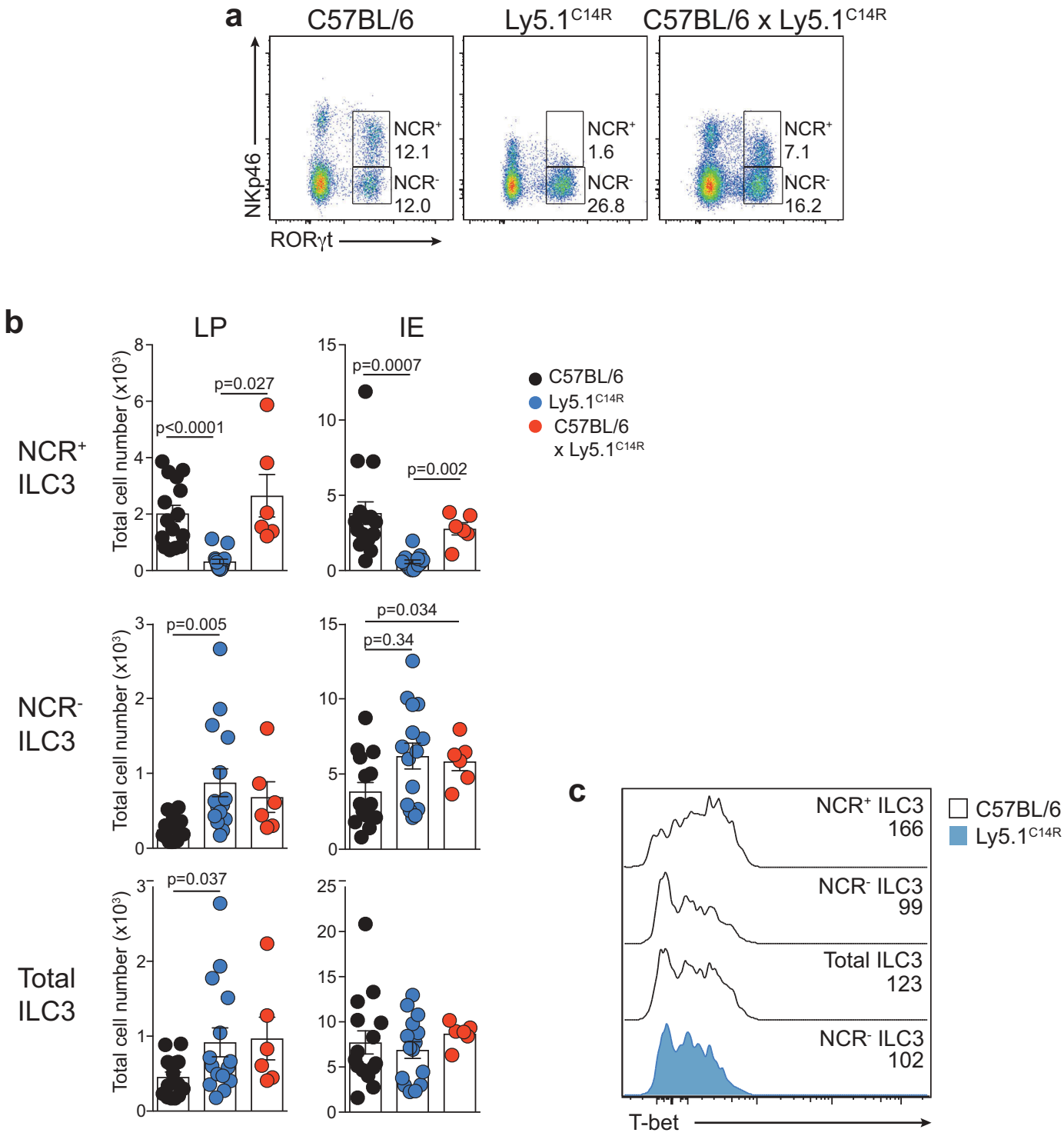


Figure 3. Ly5.1^{C14R} mice have abnormal numbers of ILC3. (A) Dot plots showing the frequency of NCR^{+} and NCR^{-} ILC3 in the LP of the small intestine of C57BL/6, Ly5.1^{C14R} and C57BL/6 × Ly5.1^{C14R} mice. Data show representative plots gated on live CD3^{-}CD19^{-} lymphocytes. (*B*) Enumeration of NCR^{+}, NCR^{-} and total ILC3 for LP and IE in the small intestine. Data showing the mean ± SEM pooled from three to six independent experiments (n = 6–15 mice/genotype). P values were calculated using an unpaired two-tailed Student's t test. (C) Histograms show the mean fluorescence intensity of intracellular staining for T-bet in ILC3 subsets from the small intestine of C57BL/6 and Ly5.1^{C14R} mice (n = 6 mice/genotype). P values were calculated using a Student's t test.

NKp46^{C14R} single point mutation developed significantly more lung metastases, a condition that was accompanied by respiratory distress. These mice also presented metastases in other organs such as the kidney, liver and bone marrow (SI Appendix, Figure S5 *D*), a phenotype which was similar to that observed in *Mcl-1$^{fl/fl}$Ncr1^{iCre}* mice in which NCR^{+} cells are conditionally ablated[29] (Figure 4C and D and SI Appendix, Figure S5D). Thus, although some function was preserved in the presence of the C14R mutation including the ability of NK cells to localize to the lung itself (SI Appendix, Figure S6), alteration of surface NKp46 in Ly5.1^{C14R} mice strongly

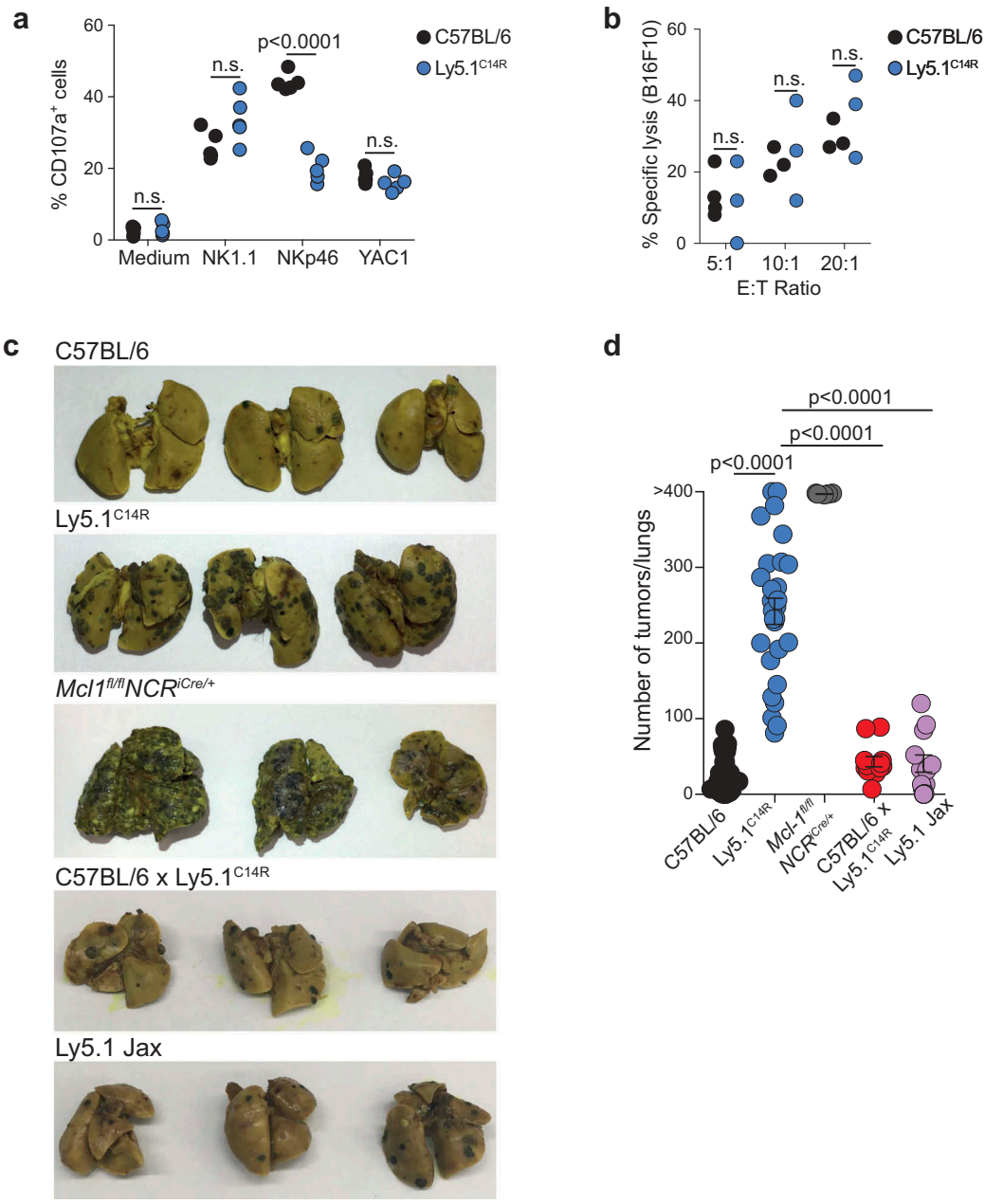


Figure 4. Ly5.1^{C14R} NK cells cells show altered sensitivity to stimuli *in vitro* but fail to control melanoma tumor development *in vivo*. (A) Degranulation capacity of total NK1.1^{+} NK cells determined by surface CD107a expression in C57BL/6 and Ly5.1^{C14R} cells. Data show frequencies of CD107a^{+} NK cells ± SEM after coculture with various stimuli. Data shown from 2 independent experiments (n = 5 mice/genotype). (B) Cytolytic activity of C57BL/6 and Ly5.1^{C14R} NK cells sensitized to B16F10 tumor cells. NK cells have been activated overnight with IL-2 (1000 U/ml). Data show the mean lysis ± SEM pooled from three independent experiments (n = 3 mice/genotype in each experiment). P values were calculated using a Student's t test. (C) Representative whole mounts of the metastatic burden in the lungs of C57BL/6, Ly5.1^{C14R}, *Mcl-1$^{fl/fl}$Ncr1^{iCre}*, C57BL/6 × Ly5.1^{C14R} and Ly5.1 (Jax, 2017) mice 14 days after i.v injection of B16F10 melanoma cells. (*D*) Total tumor burden in the lungs of C57BL/6, Ly5.1^{C14R}, *Mcl-1$^{fl/fl}$Ncr1^{iCre}*, C57BL/6 × Ly5.1^{C14R} and Ly5.1 (Jax, 2017) mice shown in (C) 14 days after injection of B16F10 melanoma cells. Data show the mean ± SEM of tumor burden pooled from five independent experiments (n = 28–30 mice/genotype). *Mcl-1$^{fl/fl}$Ncr1^{iCre}* mice included in a single experiment (n = 5 mice/genotype) while C57BL/6 × Ly5.1^{C14R} and Ly5.1 (Jax, 2016) mice were included in two experiments (n = 12 mice/genotype). P values were calculated using an unpaired two-tailed Student's t test.

impaired the capacity of NK cells to control tumor development and escape *in vivo*.

C14R mutation disrupts cellular pathways associated with protein trafficking

To further dissect the molecular alterations that underpin the changes that occur when the NKp46 expression is altered, we analysed the transcriptome of naive C57BL/6 and Ly5.1^{C14R} NK1.1^{+} NK cells by RNA-seq analyses (Figure 5, SI Appendix, Dataset S2). This revealed that there was a significant enrichment in differentially regulated genes involved in intracellular trafficking compartments including the endoplasmic reticulum, endosome, ER to Golgi vesicle-mediated transport and Golgi apparatus in Ly5.1^{C14R} cells (Figure 5A–C). In addition, alterations occurred in pathways associated with protein ubiquitination and transport together with enzymes associated with processing of proteins (eg. GTPase, peptidase activity,

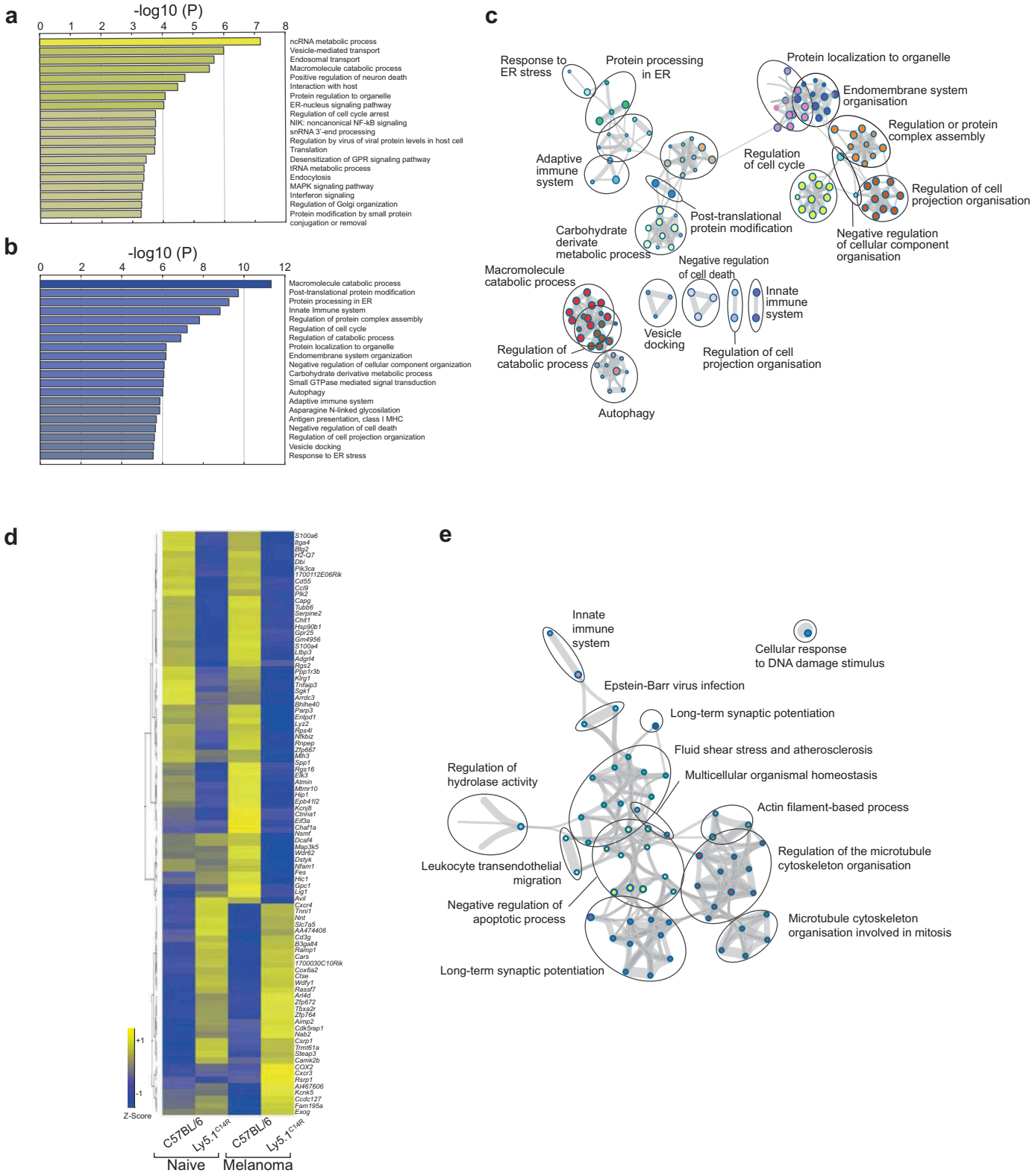


Figure 5. Altered molecular machinery in naïve Ly5.1^{C14R} mutant NK cells affects antigen processing and protein trafficking pathways. (A, B) Enrichment clusters from genes upregulated and downregulated, respectively, in naïve Ly5.1^{C14R} NK cells compared with C57BL/6 NK cells. (C) Gene ontology (GO) network analysis of significantly reduced gene expression levels in Ly5.1^{C14R} NK cells (shown in B) *via* Metascape and visualized with Cytoskape (v3.1.2). (D) Heatmap of genes significantly up and downregulated in NK cells responding to B16F10 melanoma tumor cells seven days after challenge presented to show differences in gene expression patterns for C57BL/6 and Ly5.1^{C14R} mice and the comparative gene expression found in naïve NK cells. (E) Gene ontology (GO) network analysis of significantly reduced gene expression levels in Ly5.1^{C14R} NK cells isolated from day 7 lungs of mice challenged with B16F10 tumor cells. Nodes are coloured by p-value *via* Metascape and visualized with Cytoskape.

protein kinase). Although changes to NKp46 trafficking may have been expected, consistent with a similar alteration that occurs in *Noé* mice,[20,21] broader changes in protein trafficking were not anticipated. Exome sequencing has uncovered that a broad gene set is altered in the Ly5.1^{C14R} strain that warrants further investigation.

To determine how the NKp46^{C14R} mutation might affect cells responding to a tumor challenge, we isolated total NK cells from the lungs of mice challenged with B16F10 tumor cells 7 days earlier and subjected them to RNAseq (SI Appendix, Dataset S3). Ninety-one genes were found to be differentially expressed between C57BL/6 and Ly5.1^{C14R} in NK cells in response to melanoma (Figure 5D). Genes up regulated in C14R NK cells were associated with the mitochondrion and cell differentiation, while genes involved in protein processing in the endoplasmic reticulum, transcriptional regulators and cellular organization were downregulated (Figure 5D and E). However, genes such as *Cxcr3* and *Cxcr4*, both of which are essential for infiltration and function of NK cells,[30–32] and the transcriptional regulator *Nab2* were upregulated in Ly5.1^{C14R}. We observed that in Ly5.1^{C14R} mice, the number of NK cells found in the lung were enriched ~2.1 fold indicating that the failure of tumor control was not driven by the inability to migrate to the lung.

Loss of NKp46 signaling is encoded by the point mutation C14R in Ncr1

It was clear from the analyses above that many more genes than would be anticipated are altered in Ly5.1^{C14R} mice. Thus, we could not be completely certain that the effects identified in NKp46 expression in these mice are due solely to the C14R mutation detected in the *Ncr1* gene. To determine whether this was indeed the case, we generated mice using the CRISPR/Cas9 technology[33] that would carry only the C14R mutation on a C57BL/6 background. These mice are designated as the NCR^{B6C14R} strain and were healthy, viable and bred normally to produce homozygous animals. Analyses of NKp46 surface expression in C57BL/6 and NCR^{B6C14R} mice showed that the C14R mutation alone abrogated NKp46 binding phenocopying the Ly5.1^{C14R} mice for this feature (Figure 6). Similarly, the distribution of NK cells in NCR^{B6C14R} mice were concordant with the pattern observed in Ly5.1^{C14R} mice (Figure 6B–D) while in both NCR^{B6C14R} and Ly5.1^{C14R} ILC1 were enriched in spleen and liver in four to five week old mice (Figure 6E). We also observed that NKp46^{+} ILC3 were reduced in NCR^{B6C14R} similar to that observed in Ly5.1^{C14R} mice. Notably across all organs examined, the surface expression of NKp46 was strongly reduced in NK cells and ILC1 and in blood NK cells (Figure 6F). This correlated with a strong reduction in TRAIL expression when C57BL/6 mice expressed the C14R mutation demonstrating that an alteration in NKp46 which affects the stability of the expression at the surface of the cell is sufficient to alter the induction of TRAIL in hepatic ILC1.

Discussion

Spontaneous mutations occur in eukaryotes at a rate of 0.1–100 per genome per sexual generation. In mice, nearly 5,000 spontaneous and induced mouse mutant alleles with clinically relevant phenotypes have been described in the Mouse Genome Informatics database and only about one third of these have characterized phenotypes.[34] In many cases, however, identification of these sequence alterations has served as a rich source of animal models for human genetic diseases.

Although the Ly5.1 (CD45.1) line should differ from its 'wild-type' counterpart by just five amino acids within the extracellular domain,[35] it is now clear that the *B6.SJL-Ptprca Pepcb/BoyJ* derived from Jax differs in many genes from the C57BL/6 line spanning ~40Mb and ~300 genes.[36] A single amino acid accounts for the difference between the CD45.1 and CD45.2 congenic markers that define these two strains[36] and this difference has formed the basis for their use in extensive tracking experiments. These previously unappreciated alterations in the genome have most likely impacted experimental interpretations. We now add to this list the detection of a spontaneous mutation in the *Ncr1* gene that has affected multiple mouse colonies in geographically distinct locations. This mutation may have arisen independently, but seems most likely to have arisen from an individual breeding founder from the Jax. As the C14R mutation of the *Ncr1* gene remains undetected in heterozygous animals, this mutation has inadvertently been retained undetected long term in parent colonies. Using whole exome sequencing we identified a spontaneous single autosomal recessive mutation in the *Ncr1* gene that significantly altered the expression of the NKp46 surface protein by interfering with its export to the cell surface. Subsequently, we generated C57BL/6 mice in which we introduced the C14R mutation in the *Ncr1* gene negating the effect of other genes altered in the Ly5.1^{C14R} strain. This directly confirmed that the change in NKp46 expression was solely driven by this mutation and will allow this specific mutation to be investigated in detail in future studies.

The C14R mutation in the *Ncr1* gene of the mutant Ly5.1 lines occurred just proximal to the previously reported W32R mutation in the signal peptide which can typically affect the synthesis and/or secretion of a protein.-[18,21] We show that expression of *Ncr1* mRNA was similar in NK cells of both wild-type, Ly5.1^{C14R} mouse strains suggesting that the gene is effectively transcribed but that alterations occur after this stage. The Noé strain also showed poor cell surface expression of NKp46, and like the NKp46^{C14R} NK cells, displayed no change in mRNA expression.[18] This was supported by analysis of transduced 293T cells where intracellular NKp46^{C14R} and NKp46 expression were similar, but cell surface expression was strongly impaired in NKp46^{C14R}. Genomic analyses revealed disruption in intracellular trafficking although a broader group of genes involved in transcriptional regulation and protein processing in the ER, endosome, Golgi apparatus and cellular organization were detected suggesting other potential defects in this mouse line. Collectively, however, our data suggest that in the mutants, NKp46 could be expressed on the cell surface but is unstable posing the possibility that an altered signaling pathway could be triggered by the constant internalization of NKp46. It also implies that the stability and/or level of NKp46 expression is important in signaling and prompts further dissection of the molecular control of NKp46 that appears to impact on ILC differentiation.

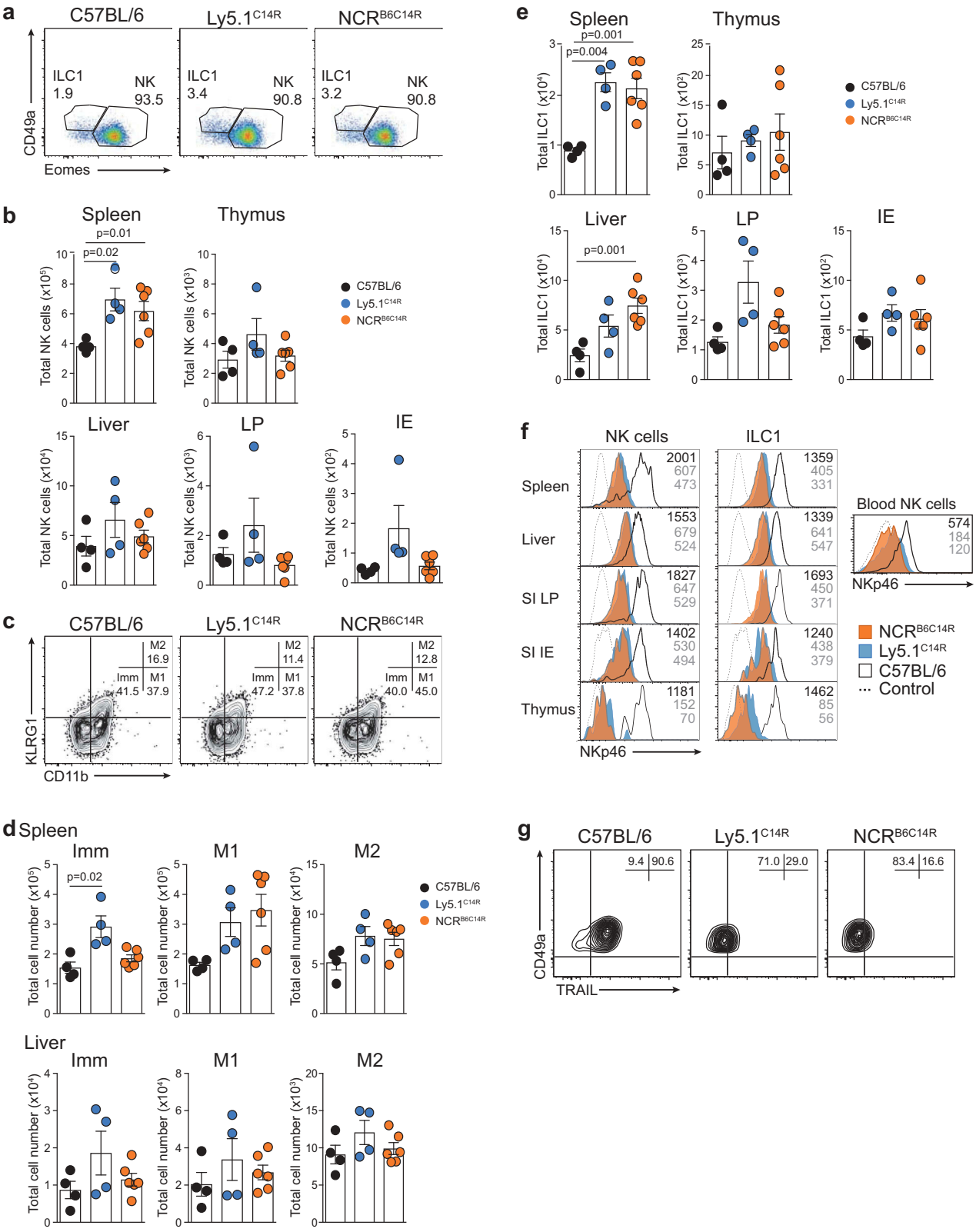


Figure 6. Loss of NKp46 surface expression depends on the C14R mutation in the *Ncr1* gene. (A) Dot plots showing the frequency of ILC1 and NK cells in the spleen. Data show representative plots gated on live NK1.1$^+$ lymphocytes excluding T and B cells. (B) Total number of NK cells in spleen, thymus, liver, small intestine lamina propria (LP) and within the intestinal intraepithelial compartment (IE). Data are pooled from two independent experiments and show the mean ± SEM (n = 4–6 mice/genotype). P values were calculated using an unpaired two-tailed Student's t test. (C) FACS plots showing the frequency of immature (Imm, KLRG1$^-$CD11b$^-$), mature 1 (M1, KLRG1$^-$CD11b$^+$) and mature 2 (M2, KLRG1$^+$CD11b$^+$) NK cells in splenic NK1.1$^+$CD3$^-$CD19$^-$ NK cells. (D) Total number of Imm, M1 and M2 NK cells in the spleen and liver of C57BL/6, Ly5.1^{C14R} and NCR^{B6C14R} mice showing the mean ± SEM pooled from two experiments (n = 4–6 mice/genotype). P values were calculated using an unpaired two-tailed Student's t test. (E) Total number of ILC1s in spleen, thymus, liver, small intestine lamina propria (LP) and within the intestinal intraepithelial compartment (IE). Data show the mean ± SEM pooled from two independent experiments (n = 4–6 mice/genotype). P values were calculated using an unpaired two-tailed Student's t test. (F) Histograms showing the mean fluorescence intensity of NKp46 in various tissues for both NK cells and ILC1 for wild-type (black solid line), Ly5.1^{C14R} (solid blue) and NCR^{B6C14R} (solid orange). CD3ε$^+$ cells were used as a control for NKp46 expression (black dashed line). Data are representative of tissues analyzed in (*A-E*). (G) Expression of TRAIL on NK1.1$^+$CD49a$^+$CD3$^-$CD19$^-$ hepatic ILC1 in C57BL/6, Ly5.1^{C14R} and NCR^{B6C14R}. Data show representative plots from two independent experiments and indicate the the frequency of expression (n = 4–6 mice/genotype).

In the Ly5.1^{C14R} mice, we observed that NK cell development in terms of cellularity was not impaired in the absence of NKp46. Neverthless, we show that the differentiation of NK cells and ILC1 were altered in both Ly5.1^{C14R} and Noé mice. NK cell subsets were skewed towards an accumulation of less mature NK cells and NCR^{-} ILC3s. The lack of NKp46 induced in *Ncr1$^{gfp/gfp}$* mice has also recently been shown to be associated with an impaired NK cell maturation in response to mouse cytomegalovirus infection (MCMV).[37] This was associated with changes in CXCR3-driven migration of NK cells to the regional lymph nodes which can affect NK-dendritic cell crosstalk necessary for priming MCMV-specific CD4^{+} T cells.[38] In our study, we found that in contrast to this observation, *Cxcr3* mRNA was upregulated, consistent with the higher expression of CXCR3 on the less mature CD27^{high}M1 NK cells.[39,40] Indeed, the number of NK cells that localized in the lung in response to a B16F10 tumor cells which are likely to express the ligand for NKp46 was not reduced in Ly5.1^{C14R} mice (SI Appendix, Figure S4) and the cytolytic machinery was intact. *Ncr1$^{gfp/gfp}$* mice appear to exhibit slightly reduced IFN-γ responses to NK1.1 stimulation *in vitro* and murine cytomegalovirus infection.[19,37] Stimulation through the NKp46 receptor has been shown to drive IFN-γ production. This NK cell-driven IFN-γ production has recently been shown to induce the extracellular matrix protein fibronectin 1 that could modulate tumor formation.[41] In contrast, diminished NKp46 appears to regulate phosphorylation of Dok-1 to influence IFN-γ production and pathogen protection.[42] In our *in vitro* analyses, a reduction in IFN-γ was not observed in our mutant mice although signaling directly through NKp46 was strongly impaired. Thus, it appears that the complete loss of function of the *Ncr1* allele in *Ncr1$^{gfp/gfp}$* mice differs from the disruption induced by the introduction of a point mutation in the gene.

In addition to changes in NK cell differentiation, we observed that diminished NKp46 expression caused alterations in other ILCs. Although loss of NKp46 did not impair ILC1 numbers, we show that the apoptosis-inducing ligand TRAIL, which can be induced by TGF-β[43] and through viral binding to NKp46[44] was lacking implying that NKp46 may play a role in regulating TRAIL expression. NKp46 is also a key marker of one of the three subsets of ILC3.[18] In Ly5.1^{C14R} mice, as expected NCR^{+} ILC3 were not detectable *via* NKp46 expression but we also did not see enrichment of expression of T-bet which is normally associated with induction of this subset,[25,26] although ILC3 development itself was not affected implying that activation of NKp46 is important for the transcriptional program of these cells. This is supported by cell fate mapping experiments that suggest that instability of NKp46 expression in ILC3s found in the intestine reflects a major role of this receptor in tuning the very dynamic environmental signals encountered that drive ILC3 plasticity.[45,46] Loss of *Ncr1* has previously been shown not to affect ILC3 development with *Ncr1$^{gfp/gfp}$Rag2$^{-/-}$* mice showing survival and clinical scores similar to control mice when challenged with the enteric infection *Citrobacter rodentium*.[47] In this setting, NKp46 expression did not appear to be essential for protection.

In summary, we have identified a commonly used mouse line, the Ly5.1^{C14R}, that carries a point mutation in the *Ncr1* gene together with a large number of previously unknown genes. The NCR^{B6C14R} strain confirmed that the C14R *Ncr1* mutation directly impaired the expression of surface NKp46 and alters differentiation of NK cells with increased accumulation of immature stages. In addition, increased numbers of ILC1 were found and these cells lacked TRAIL expression while NCR^{+} ILC3 were not detected. Thus, although reduced NKp46 expression did not disrupt either NK cell or ILC development, it exerted an important impact on normal differentiation, maturation and activation of these lineages.

Materials and methods

Mice

C57BL/6 and *B6.SJL-Ptprca Pepcb/BoyJ* (Ly5.1, originally obtained from The Jackson Laboratory), C57BL/6 × *B6.SJL-PtprcaPepcb/BoyJ* (C57BL/6 × Ly5.1 and *B6.SJL-Ptprca Pepcb/BoyJAX* (imported 2016 and sequence verified) mice were bred and maintained in-house at either the Walter and Eliza Hall Institute of Medical Research (WEHI, Australia) or the University Hospital Erlangen (Germany) under specific pathogen-free conditions. Mice used in Frankfurt were obtained from the Preclinical Experimental Animal Center (PETZ) of the Friedrich Alexander University (FAU) Erlangen-Nürnberg, Germany. *Ncr1$^{gfp/gfp}$*, *Noé* mice and *Mcl1$^{fl/fl}$Ncr1^{iCre}* mice have been previously described.[17,18,29] CD45.1^{STEM} mice[36] were bred at the Massachusetts General Hospital animal house (Boston). Male and female mice were used between the ages of six to eight weeks and were age matched unless otherwise stated. NCR^{B6C14R} mice were used at four to five weeks of age. Animal experiments followed the National Health and Medical Research Council (NHMRC) Code of Practice for the Care and Use of Animals for Scientific Purposes guidelines and were approved by the Animal Ethics Committee of the respective institutions.

Generation of NCR^{B6C14R} mice

A new C57BL/6 mouse strain that carried the C14R mutation in the *Ncr1* gene (NCR^{B6C14R}) was generated using CRISPR/Cas9 as previously described.[33] Briefly, one sgRNA of the sequence TAGGGCTATGTCTGAGCCAG (10ng/μl), an oligo donor of the sequence (gttgaatcaagagcagattgggggag acagcatgccattaaccctgttttctagGGCTACGACTGAGCCAGCGT-ATCAACACTGAAAAGGgtaagtccttccctcgaagtctcagggttgttctt-atgggttca; 10ng/ul) and Cas9 mRNA (5ng/μl) were injected into the cytosol of C57BL/6J zygotes to generate NCR^{B6C14R} point mutant mice.

Generation of mixed bone marrow chimeric mice

Mixed bone marrow chimeric mice were generated by reconstituting lethally irradiated (2 x 5.5Gy γ-irradiation, ^{137}Cs source) with a mixture (1:1 ratio; total 10 × 10^{6} bone marrow cells/mouse) of Ly5.1^{C14R} (CD45.1$^{+/+}$) and C57BL/6

× Ly5.1^{C14R} (CD45.2^{+}CD45.1^{+}) bone marrow. Mice were analysed 6–8 wk after reconstitution.

Isolation of intestinal intraepithelial and lamina propria lymphocytes

Intestinal LPL were isolated from the intestine as previously described.[26,48]

Cell isolation and flow cytometric analyses

Single cell suspensions were generated by forcing organs through 70 µm sieves. Lymphocytes were isolated from liver using a 33% isotonic Percoll (Amersham Pharmacia Biotech) gradient centrifuged at 2000 rpm for 13 min at ambient temperature. Single cell suspensions were blocked with PBS containing 5 µg/ml anti-CD16/CD32 (2.4G2) and stained for 20–30 min on ice with fluorophore-conjugated antibodies, unless stated otherwise. For analysis of surface molecules, cells were stained with the following antibodies: anti-CD11b (M1/70) (BD Biosciences, or Miltenyi), anti-CD3ε (145-2C11) and anti-CD19 (1D3 and 6D5) (BioLegend), anti-KLRG1 (2F1), and anti-NK1.1 (PK136), anti-CD27 (LG.3A11), anti-CD45.1 (A20), anti-CD45.2 (104), anti-CD49a (HMα1), anti-B220 (RA3-6B2) (all from BD Biosciences), anti-NKp46 (29A1.4, eBioscience) and anti-CD49b (DX5, generated at The Walter and Eliza Hall Institute hybridoma facility). Live cells were identified by exclusion after staining with a fixable viability dye (BD Biosciences or BioLegend). Intracellular staining was performed using the Transcription Factor Staining Buffer Set (eBioscience) and monoclonal antibodies to EOMES (Dan11mag), GATA3 (TWAJ) (both from eBioscience) and RORγt (Q31-378, BD Biosciences). For IFN-γ detection, the monoclonal antibody XMG1.2 (BD Pharmingen) was used. Flow cytometry was performed using a LSRFortessa X-20 or Canto10C (BD Biosciences) and FlowJo analysis software (Treestar).

Murine melanoma cells and pulmonary metastasis

B16F10 murine melanoma cells (mycoplasma negative) were maintained in complete DMEM (Gibco) with 10% heat-inactivated FCS, 2 mM of L-Glutamine, 100 U/mL penicillin, and 100 µg/mL streptomycin. 2.5×10^5 B16F10 cells were injected into the tail vein of recipient mice. Fourteen days after injection, the lungs, liver, long bones and kidneys were harvested and fixed in Bouin's solution. B16F10 metastases were counted using a dissecting microscope.[49]

Exome sequencing

To identify the genetic mutation responsible for the reduced NKp46 expression in the Ly5.1^{C14R} strain we performed exome sequencing on two mice from this strain and the C57BL/6 × Ly5.1^{C14R} mice which expressed normal NKp46 protein levels (SI Appendix, Methods).

Sanger sequencing

To further confirm the Ncr1 mutation identified by exome sequencing we performed Sanger sequencing on C57BL/6, C57BL/6 × Ly5.1 and WEHI *B6.SJL-Ptprca Pepcb/BoyJ* mice (SI Appendix, Methods).

Quantitative PCR

RNA was isolated from sorted NK cells and NKp46 expression was determined as described in SI Appendix, Methods.

Cloning

NKp46 cDNA were generated from RNA isolated from purified NK cells of either C57BL/6 or Ly5.1^{C14R} mice by RT-PCR and cloned into the plasmid RSV.5neo-FlagHis which provides C-terminal FLAG- and hexahistidine-tags.

Primers: NKp46 cDNA forward 5′-GACTCCGCG GGCCACCATGCTGCCAACACTCACTG-3′, NKp46 cDNA reverse 5′-AGTCCTCGAG CAAGGCCCCAGGAGTTGC-3′.

Transfection and flow cytometric analysis

293T cells were cultured in Dulbecco's Modified Eagle's Medium and were transfected with the appropriate RSV.5neo expression vectors containing NKp46 WT or mutant cDNA with Flag- and hexahistidine-tag using Applifect (AppliChem) (SI Appendix, Methods). Cells were fixed and permeabilized with BD Cytofix/Cytoperm (BD Biosciences) and subsequently stained with appropriate antibodies for 20 min at 4°C. Antibodies used: FLAG-tag mAb M2 (Sigma), anti-NKp46-PE mAb 29A1.4 (BioLegend), rat IgG2a-PE isotype control RTK2758 (BioLegend), mouse IgG1 isotype control N1G9, APC-conjugated F(ab)2-fragments of goat anti-mouse IgG (Jackson ImmunoResearch). Flow cytometry analysis was performed with a FACS Canto II (BD Biosciences, Heidelberg, Germany) and data analyzed using FlowJo (Tree Star, Ashland, OH).

Immunofluorescence staining

NK cells were isolated from the spleens of Ly5.1^{C14R} and C57BL/6 mice and centrifuged on lysine coated slides, then fixed and stained with goat anti-mouse NKp46 antibody (R&D Systems, AF2225, 1:100) and rabbit anti-mouse PDI (Cell Signaling Technology, 3501S, 1:100) overnight, followed by AlexaFluor488-conjugated donkey anti-goat IgG (H + L) (ThermoFisher, A-11055, 1:250) and AlexFluor546-conjugated donkey anti-rabbit IgG (H + L) (ThermoFisher, A-10040, 1:200). Images were analyzed using LAS AF (Leica Application Suite – Advanced Fluorescence) software (SI Appendix, Methods).

NK cell stimulation

Plates were coated overnight at 4°C with antibodies against NK1.1 and NKp46 (10 µg/ml in PBS). 1.5×10^6 splenocytes were cultured in 200µl of complete RPMI1640 media

containing 10% heat-inactivated FCS, 2mM of L-Glutamine, 100 U/mL penicillin, and 100 µg/mL streptomycin in the presence of Golgi Stop and soluble CD107a for 4h at 37°C. The YAC1 stimulation condition was obtained by adding 0.25 10^6 YAC1 cells to the well. Cells were subsequently stained and analyzed by flow cytometry with an LSR Fortessa and data analyzed using FlowJo (Tree Star, Ashland, OH).

Cytotoxicity assay

Europium release assay was used to assess the lytic capacity of murine NK cells as described in SI Appendix, Methods.

RNA-seq analysis

RNA-seq analyses was performed on NK cells isolated from the lungs of Ly5.1^{C14R} and C57BL/6 mice seven days after challenge with B16F10 melanoma tumor cells. These strains were sourced from the sourced from the WEHI colonies. Samples were sequenced on an Illumina NextSeq 500 generating 75 bp paired end reads. Two biological replicates of each cell type were sequenced. RNA-seq Reads were aligned to the GRCm38/mm10 build of the Mus musculus genome using the Subread aligner.[50] Only uniquely mapped reads were retained. Genewise counts were obtained using featureCounts.[51] Reads overlapping exons in annotation build 38.1 of NCBI RefSeq database were included. Genes were excluded from downstream analysis if they failed to achieve a CPM (counts per million mapped reads) value of greater than 0.5 in at least two libraries. Counts were converted to log2 counts per million, quantile normalized and precision weighted with the voom function of the limma package.[52,53] A linear model was fitted to each gene, and empirical Bayes moderated t-statistics were used to assess differences in expression.[54] A false discovery rate cut-off of 0.15 was applied for calling differentially expressed genes. Gene Ontology and gene enrichment analyses were performed using Metascape (http://metascape.org). Raw data files for the RNA sequencing have been deposited in the NCBI Gene Expression Omnibus under accession number GSE113030.

Highlights

- A spontaneous mutation in the signal sequence of the *Ncr1* gene arose in the CD45.1 mouse strain
- *Ncr1* C14R mutation impairs NKp46 surface expression in NK cells, ILC1 and ILC3
- Destabilization of *Ncr1* by the C14R mutation results in accumulation of NKp46 in the endoplasmic reticulum
- Loss of stable NKp46 expression impairs the maturation of NKp46$^+$ ILCs and impairs tumor control

Acknowledgments

We thank M. Camilleri, J. Janssen, S. Cree, C. O'Brien and A. Abendroth and K. Stein for expert technical support and Dr J. Babon for helpful discussions, and Prof. C. Bogdan for providing mice and helpful discussion of results. This study was made possible through Victorian State Government Operational Infrastructure Support and Australian Government NHMRC Independent Research Institute Infrastructure Support Scheme (Walter and Eliza Hall Institute of Medical Research) and the LOEWE Center for Cell and Gene therapy (to ST and EU), Frankfurt, funded by the Hessian Ministry of Higher Education, Germany (III L 4-518/17.004).

Funding

This work was supported by the National Health and Medical Research Council Australia [1054925]; and the National Health and Medical Research Council Australia [1124907]. E.U. lab has been supported by the LOEWE Center for Cell and Gene Therapy Germany [III L 4-518/17.004]. S.U. lab is supported by funding form the European Research Council (ERC) under the European Union's Horizon 2020 research and innovation programme under grant agreement No 648768; from the ANR (No ANR-14-CE14-0009-01) and from the fondation ARC (No PGA120140200817). E.V. lab is supported by funding form the European Research Council (ERC) under the European Union's Horizon 2020 research and innovation programme (TILC, grant agreement N° 694502); the Agence Nationale de la Recherche; Equipe Labellisée "La Ligue," Ligue Nationale contre le Cancer, MSDAvenir, Innate Pharma and institutional grants to the CIML (INSERM, CNRS, and Aix-Marseille University) and to Marseille Immunopôle. S.T. received a GO-IN postdoc fellowship at the University Frankfurt Germany [PCOFUND-GA-2011-291776] and by the Madeleine Schickedanz-KinderKrebs-Stiftung; W.S. is supported by a Walter and Eliza Hall Institute Centenary Fellowship sponsored by CSL Limited. S.N.W. was supported by a Walter and Eliza Hall Trust Centenary Fellowship.

Declaration of interest statement

E.V. is cofounder and employee of Innate Pharma.

Authors Contributions

M.E.F., S.W., A.G., T.Z., T.W., J.K., A.S., A.M., F.G., S.U., E.N-M., B.R., F.S., F.F., S.T., M.A.F., J.G., S.N.W., K.L., A.G.C. and F.F.A performed experiments and analysed data; M.H. and A.K. helped create the NCR^{B6C14R} mice. T.W., U.S., J.K., A.S., N.D.H., F.E.M, D.T.S., E.U., E. V. and G.T.B. provided intellectual input and tools or reagents; A.G., Y.L. and W.S. performed bioinformatics analyses. G.T.B. and E.U. conceived the ideas and interpreted data; G.T.B, E.U., F.F.A. and S.T. wrote the paper and edited it with the assistance of the other authors.

ORCID

Francisca F. Almeida http://orcid.org/0000-0001-6632-7610
Sophie Ugolini http://orcid.org/0000-0003-4041-0103
Alexander Steinle http://orcid.org/0000-0001-5081-8503
Eric Vivier http://orcid.org/0000-0001-7022-8287
Gabrielle T. Belz http://orcid.org/0000-0002-9660-9587
Evelyn Ullrich http://orcid.org/0000-0001-8530-1192

References

1. Lam VC, Lanier LL. NK cells in host responses to viral infections. Curr Opin Immunol. 2017;44:43–51. doi:10.1016/j.coi.2016.11.003.
2. Vivier E, Tomasello E, Baratin M, Walzer T, Ugolini S. Functions of natural killer cells. Nat Immunol. 2008;9(5):503–510. doi:10.1038/ni1582.
3. Seidel E, Glasner A, Mandelboim O. Virus-mediated inhibition of natural cytotoxicity receptor recognition. Cell Mol Life Sci. 2012;69(23):3911–3920. doi:10.1007/s00018-012-1001-x.
4. Thielens A, Vivier E, Romagne F. NK cell MHC class I specific receptors (KIR): from biology to clinical intervention. Curr Opin Immunol. 2012;24(2):239–245. doi:10.1016/j.coi.2012.01.001.

5. Satoh-Takayama N, et al.. Microbial flora drives interleukin 22 production in intestinal NKp46+ cells that provide innate mucosal immune defense. Immunity. 2008;29(6):958–970. doi:10.1016/j.immuni.2008.11.001.
6. Luci C, et al.. Influence of the transcription factor RORgammat on the development of NKp46+ cell populations in gut and skin. Nat Immunol. 2009;10(1):75–82. doi:10.1038/ni.1681.
7. Sanos SL, Bui VL, Mortha A, Oberle K, Heners C, Johner C, Diefenbach A. RORγt and commensal microflora are required for the differentiation of mucosal interleukin IL22-producion NKp46+ cells. Nature Immunology. 2009;10(1):83–91. doi:10.1038/ni.1684.
8. Narni-Mancinelli E, et al.. Complement factor P is a ligand for the natural killer cell-activating receptor NKp46. Sci Immunol. 2017;2:10. doi:10.1126/sciimmunol.aam9628.
9. Vankayalapati R, et al.. The NKp46 receptor contributes to NK cell lysis of mononuclear phagocytes infected with an intracellular bacterium. J Immunol. 2002;168(7):3451–3457. doi:10.4049/jimmunol.168.7.3451.
10. Mandelboim O, et al.. Recognition of haemagglutinins on virus-infected cells by NKp46 activates lysis by human NK cells. Nature. 2001;409(6823):1055–1060. doi:10.1038/35059110.
11. Draghi M, et al.. NKp46 and NKG2D recognition of infected dendritic cells is necessary for NK cell activation in the human response to influenza infection. J Immunol. 2007;178(5):2688–2698. doi:10.4049/jimmunol.178.5.2688.
12. Arnon TI, et al.. Recognition of viral hemagglutinins by NKp44 but not by NKp30. Eur J Immunol. 2001;31(9):2680–2689. doi:10.1002/1521-4141(200109)31:9<2680::AID-IMMU2680>3.0.CO;2-A.
13. Jarahian M, et al.. Activation of natural killer cells by newcastle disease virus hemagglutinin-neuraminidase. J Virol. 2009;83(16):8108–8121. doi:10.1128/JVI.00211-09.
14. Jarahian M, et al.. Modulation of NKp30- and NKp46-mediated natural killer cell responses by poxviral hemagglutinin. PLoS Pathog. 2011;7(8):e1002195. doi:10.1371/journal.ppat.1002195.
15. Chaushu S, et al.. Direct recognition of Fusobacterium nucleatum by the NK cell natural cytotoxicity receptor NKp46 aggravates periodontal disease. PLoS Pathog. 2012;8(3):e1002601. doi:10.1371/journal.ppat.1002601.
16. Vitenshtein A, et al.. NK cell recognition of candida glabrata through binding of NKp46 and NCR1 to fungal ligands Epa1, Epa6, and Epa7. Cell Host Microbe. 2016;20(4):527–534. doi:10.1016/j.chom.2016.09.008.
17. Gazit R, et al.. Lethal influenza infection in the absence of the natural killer cell receptor gene Ncr1. Nat Immunol. 2006;7(5):517–523. doi:10.1038/ni1322.
18. Narni-Mancinelli E, et al.. Tuning of natural killer cell reactivity by NKp46 and Helios calibrates T cell responses. Science. 2012;335(6066):344–348. doi:10.1126/science.1215621.
19. Sheppard S, et al.. Characterization of a novel NKG2D and NKp46 double-mutant mouse reveals subtle variations in the NK cell repertoire. Blood. 2013;121(25):5025–5033. doi:10.1182/blood-2012-12-471607.
20. Glasner A, et al.. Expression, function, and molecular properties of the killer receptor Ncr1-Noe. J Immunol. 2015;195(8):3959–3969. doi:10.4049/jimmunol.1501234.
21. Glasner A, Isaacson B, Mandelboim O. Expression and function of NKp46 W32R: the human homologous protein of mouse NKp46 W32R (Noe). Sci Rep. 2017;7:40944. doi:10.1038/srep40944.
22. Walzer T, et al.. Identification, activation, and selective in vivo ablation of mouse NK cells via NKp46. Proc Natl Acad Sci U S A. 2007;104(9):3384–3389. doi:10.1073/pnas.0609692104.
23. Gordon SM, et al.. The transcription factors T-bet and Eomes control key checkpoints of natural killer cell maturation. Immunity. 2012;36(1):55–67. doi:10.1016/j.immuni.2011.11.016.
24. Seillet C, et al.. Differential requirement for Nfil3 during NK cell development. J Immunol. 2014;192(6):2667–2676. doi:10.4049/jimmunol.1302605.
25. Klose CS, et al.. A T-bet gradient controls the fate and function of CCR6-RORgammat+ innate lymphoid cells. Nature. 2013;494(7436):261–265. doi:10.1038/nature11813.
26. Rankin LC, et al.. The transcription factor T-bet is essential for the development of NKp46(+) innate lymphocytes via the Notch pathway. Nat Immunol. 2013;14(4):389–395. doi:10.1038/ni.2545.
27. Grundy MA, Zhang T, Sentman CL. NK cells rapidly remove B16F10 tumor cells in a perforin and interferon-gamma independent manner in vivo. Cancer Immunol Immunother. 2007;56(8):1153–1161. doi:10.1007/s00262-006-0264-1.
28. Smyth MJ, et al.. Differential tumor surveillance by natural killer (NK) and NKT cells. J Exp Med. 2000;191(4):661–668. doi:10.1084/jem.191.4.661.
29. Sathe P, et al.. Innate immunodeficiency following genetic ablation of Mcl1 in natural killer cells. Nat Commun. 2014;5:4539. doi:10.1038/ncomms5539.
30. Noda M, et al.. CXCL12-CXCR4 chemokine signaling is essential for NK-cell development in adult mice. Blood. 2011;117(2):451–458. doi:10.1182/blood-2010-04-277897.
31. Bernardini G, Antonangeli F, Bonanni V, Santoni A. Dysregulation of chemokine/chemokine receptor axes and NK cell tissue localization during diseases. Front Immunol. 2016;7:402. doi:10.3389/fimmu.2016.00402.
32. Pak-Wittel MA, Yang L, Sojka DK, Rivenbark JG, Yokoyama WM. Interferon-gamma mediates chemokine-dependent recruitment of natural killer cells during viral infection. Proc Natl Acad Sci U S A. 2013;110(1):E50–59. doi:10.1073/pnas.1220456110.
33. Wang H, et al.. One-step generation of mice carrying mutations in multiple genes by CRISPR/Cas-mediated genome engineering. Cell. 2013;153(4):910–918. doi:10.1016/j.cell.2013.04.025.
34. Blake JA, et al.. The Mouse Genome Database (MGD): premier model organism resource for mammalian genomics and genetics. Nucleic Acids Res. 2011;39(Database issue):D842–848. doi:10.1093/nar/gkq1008.
35. Zebedee SL, Barritt DS, Raschke WC. Comparison of mouse Ly5a and Ly5b leucocyte common antigen alleles. Dev Immunol. 1991;1(4):243–254. doi:10.1155/1991/52686.
36. Mercier FE, Sykes DB, Scadden DT. Single targeted exon mutation creates a true congenic mouse for competitive hematopoietic stem cell transplantation: the C57BL/6-CD45.1(STEM) mouse. Stem Cell Reports. 2016;6(6):985–992. doi:10.1016/j.stemcr.2016.04.010.
37. Miletic A, et al.. NCR1-deficiency diminishes the generation of protective murine cytomegalovirus antibodies by limiting follicular helper T-cell maturation. Eur J Immunol. 2017. doi:10.1002/eji.201646763.
38. Mandaric S, et al.. IL-10 suppression of NK/DC crosstalk leads to poor priming of MCMV-specific CD4 T cells and prolonged MCMV persistence. PLoS Pathog. 2012;8(8):e1002846. doi:10.1371/journal.ppat.1002846.
39. Hayakawa Y, Smyth MJ. CD27 dissects mature NK cells into two subsets with distinct responsiveness and migratory capacity. J Immunol. 2006;176(3):1517–1524. doi:10.4049/jimmunol.176.3.1517.
40. Meinhardt K, et al.. Identification and characterization of the specific murine NK cell subset supporting graft-versus-leukemia- and reducing graft-versus-host-effects. Oncoimmunology. 2015;4(1):e981483. doi:10.4161/2162402X.2014.981483.
41. Glasner A, et al.. NKp46 receptor-mediated interferon-g production by natural killer cells increases fibronectin 1 to alter tumor architecture and control metastasis. Immunity. 2018;48:1–13. doi:10.1016/j.immuni.2017.12.007.
42. Jang Y, et al.. Cutting edge: check your mice-A point mutation in the Ncr1 locus identified in CD45.1 congenic mice with consequences in mouse susceptibility to infection. J

Immunol. 2018;200(6):1982–1987. doi:10.4049/jimmunol.1701676.
43. Cortez VS, et al.. Transforming growth factor-beta signaling guides the differentiation of innate lymphoid cells in salivary glands. Immunity. 2016;44(5):1127–1139. doi:10.1016/j.immuni.2016.03.007.
44. Liang Y, et al.. The hemagglutinin-neuramidinase protein of Newcastle disease virus upregulates expression of the TRAIL gene in murine natural killer cells through the activation of Syk and NF-kappaB. PLoS One. 2017;12(6):e0178746. doi:10.1371/journal.pone.0178746.
45. Viant C, et al.. Transforming growth factor-beta and Notch ligands act as opposing environmental cues in regulating the plasticity of type 3 ILCs. Sci Signal. 2016;9(426):ra46. doi:10.1126/scisignal.aaf2176.
46. Verrier T, et al.. Phenotypic and functional plasticity of murine intestinal NKp46+ group 3 innate lymphoid cells. J Immunol. 2016;196(11):4731–4738. doi:10.4049/jimmunol.1502673.
47. Satoh-Takayama N, et al.. The natural cytotoxicity receptor NKp46 is dispensable for IL-22-mediated innate intestinal immune defense against Citrobacter rodentium. J Immunol. 2009;183(10):6579–6587. doi:10.4049/jimmunol.0901935.
48. Rankin LC, et al.. Complementarity and redundancy of IL-22-producing innate lymphoid cells. Nat Immunol. 2016;17(2):179–186. doi:10.1038/ni.3332.
49. Ferrari de Andrade L, et al.. Natural killer cells are essential for the ability of BRAF inhibitors to control BRAFV600E-mutant metastatic melanoma. Cancer Research. 2014;74(24):7298–7308. doi:10.1158/0008-5472.CAN-14-1339.
50. Liao Y, Smyth GK, Shi W. The subread aligner: fast, accurate and scalable read mapping by seed-and-vote. Nucleic Acids Res. 2013;41(10):e108. doi:10.1093/nar/gkt214.
51. Liao Y, Smyth GK, Shi W. featureCounts: an efficient general purpose program for assigning sequence reads to genomic features. Bioinformatics. 2013.
52. Law CW, Chen Y, Shi W, Smyth GK. voom: precision weights unlock linear model analysis tools for RNA-seq read counts. Genome Biol. 2014;15(2):R29. doi:10.1186/gb-2014-15-2-r29.
53. Ritchie ME, et al.. limma powers differential expression analyses for RNA-sequencing and microarray studies. Nucleic Acids Res. 2015;43(7):e47. doi:10.1093/nar/gkv007.
54. Smyth GK. Linear models and empirical bayes methods for assessing differential expression in microarray experiments. Stat Appl Genet Mol Biol. 2004;3. Article3. doi:10.2202/1544-6115.1027.